ELSEVIER

Journal of Structural Geology 26 (2004) 435–449

JOURNAL OF STRUCTURAL GEOLOGY

www.elsevier.com/locate/jsg

Late pervasive crustal-scale extension in the south Armorican Hercynian belt (Vendée, France)

Florence Cagnard*, Denis Gapais, Jean Pierre Brun, Charles Gumiaux, Jean Van den Driessche

Géosciences Rennes, UMR 6118 CNRS, Université de Rennes 1, 35042 Rennes cedex, France

Received 17 January 2003

Abstract

The coast of Vendée, in the southern Hercynian Armorican Massif, shows a complete Barrovian metamorphic section, from upper-crustal low-grade metasediments, down to high-grade partially molten rocks. The bottom of the pile is intruded by numerous synkinematic granitic dykes. The pattern of the dyke array shows that syn-emplacement deformation combined coaxial sub-vertical shortening and sub-horizontal shearing. Strain estimates using dykes and deformed metamorphic isograds suggest a maximum amount of bulk shortening in the range of 80%. Results are consistent with extensional tectonics mainly accommodated by large pervasive thinning, rather than by strain localisation along a detachment zone.

Keywords: Crustal-scale extension; Strain analysis; Dyke array; Hercynian belt; Brittany; France

1. Introduction

Post-thickening thermal reequilibration creates conditions suitable for spreading-type lithosphere-scale extension (e.g. Coney and Harms, 1984; England and Thompson, 1984; Sonder et al., 1987). In general, extension implies pervasive spreading of the ductile crust, as illustrated by the Basin and Range Province or the Aegean Domain ('wide rift' extension; Buck, 1991) (Fig. 1a). In the brittle crust, this spreading-type extension mode is expressed by distributed block faulting. Where strain localisation occurs in the brittle crust, rise-up of the ductile crust below detachment zones produces 'core complexes' (Fig. 1b) (e.g. Davis and Coney, 1979; Crittenden et al., 1980) that can be viewed as local anomalies within a more distributed extension field (Brun et al., 1994). Block faulting develops during the whole history; whereas core complexes generally characterize the early stages of extension (e.g. Coney and Harms, 1984; Kliegfield and Crespi, 1984). Since the end of the 1970s, a considerable literature has discussed brittle and ductile deformations related to 'core complex' formation, especially in recent orogens. In contrast, because exhumation of the lower crust can require much more long term erosion in the case of 'wide rift' mode, characteristics and mechanisms of associated ductile deformation are poorly documented.

In the Hercynian belt of Western Europe, widespread post-thickening extension, including detachment zones and extensional gneiss domes, has been recently documented (see Burg et al. (1994) and references therein). The present paper discusses extensional processes observed in the internal zones of the Hercynian Belt of Brittany. The study is focussed on the Sables d'Olonne area, in Vendée (Fig. 2), where no evidence of detachment is observed. In this area, the possible occurrence of extensional deformations has already been invoked (Gapais et al., 1993; Geoffroy, 1993; Burg et al., 1994; Colchen and Rolin, 2001), but no tectonic model has been proposed.

Several works have shown interest in the geometric analysis of dyke arrays for strain analysis, because of their various attitudes with respect to principal strains (Watterson, 1968; Talbot, 1970; Escher and Watterson, 1974; Escher et al., 1975; Passchier, 1990). In the present paper, we first document the occurrence of crustal extension in the area using an analysis of a synkinematic array of granitic dykes. Then, the amount of extension is estimated using both dyke patterns and deformed metamorphic isograds.

* Corresponding author. Tel.: +33-1-23-23-67-83; fax: +33-1-23-23-67-36.

E-mail address: florence.cagnard@univ-rennes1.fr (F. Cagnard).

0191-8141/$ - see front matter © 2003 Elsevier Ltd. All rights reserved.
doi:10.1016/j.jsg.2003.08.006

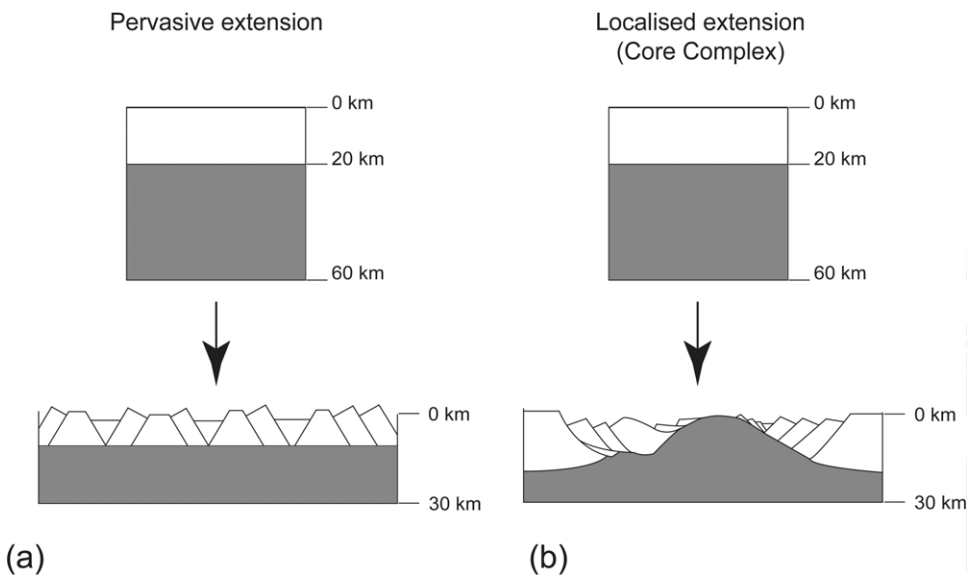

Fig. 1. Sketch illustrating two end-member processes of crustal extension, pervasive horizontal thinning (a) or localised detachment inducing core-complex development (b).

2. Geological setting

The South Brittany Domain (Fig. 2) belongs to the internal zones of the Hercynian Belt of Western Europe. It is bounded to the North by a major dextral wrench zone, the South Armorican Shear Zone (SASZ) (Jégouzo, 1980). In South Brittany, main geological units are as follows (Fig. 2):

- Uppermost units are marked by metamorphic histories of HP–LT type. They are from top to bottom: (1) blueschists (Bois de Céné and Ile de Groix blueschists,

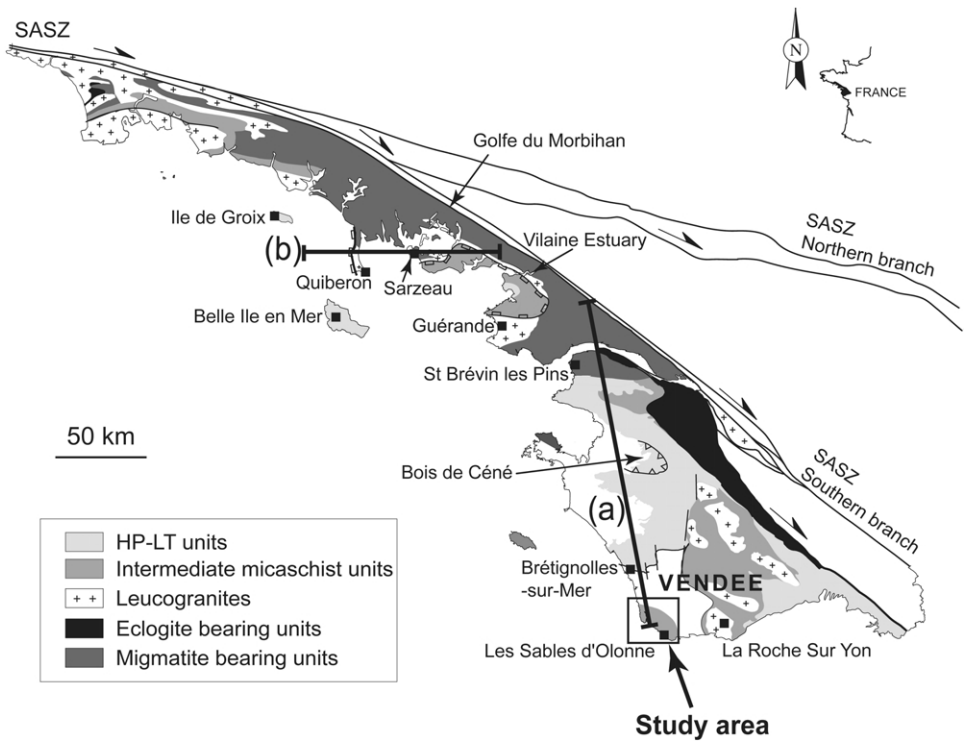

Fig. 2. Simplified geological map of the South Armorican Domain and location of the study area, along the Vendée coast, between Brétignolles-sur-Mer and Les Sables d'Olonne. Cross-sections (a) and (b) are shown on Fig. 3. SASZ is South Armorican Shear Zone.

1400–1900 MPa, 500–550 °C; Bosse et al., 2002 and references therein), and (2) metamorphosed volcanics and black shales (Vendée and Belle-Ile-en-Mer porphyroids, 700–900 MPa, 350–400 °C; Le Hébel et al., 2002).

- Intermediate units mainly consist of micaschists marked by Barrovian metamorphism, increasing downward from greenschist facies to amphibolite facies conditions (Triboulet and Audren, 1988; Goujou, 1992 and references therein).
- Lowermost units consist of high-grade rocks, with large volumes of migmatites. Local estimates of peak metamorphic conditions have yielded values of the order of 700–750 °C and 1000 MPa (Golfe du Morbihan area; Jones and Brown, 1990).

Recent geochronological studies have shown that these units can be grouped into two main sets. Ar–Ar analyses on white micas from the HP–LT units have yielded Lower-Carboniferous cooling ages around 350 Ma (Bosse et al., 2002; Le Hébel, 2002). In contrast, data available in the HT units point to a major Upper-Carboniferous event. In the Golfe du Morbihan migmatites, cooling occurred between about 310 and 290 Ma (U/Pb on monazites, Ar–Ar on hornblendes and white micas, Rb/Sr on biotites; Gapais et al., 1993; Brown and Dallmeyer, 1996). In Vendée, Ar–Ar data on white micas indicate cooling around 310 Ma (Goujou, 1992).

Several sheets or laccoliths of two-mica granites are emplaced below the HP–LT group, generally within the micaschists (e.g. Quiberon, Sarzeau, or Guérande granites). Available ages indicate that they emplaced and cooled between 310 and 300 Ma (Bernard-Griffiths et al., 1985; Le Corre et al., 1991; Le Hébel, 2002).

At regional-scale, the overall structural pattern of South Brittany is that of migmatite-rich windows overlain by lower temperature domains (Fig. 2). In the migmatite cores, the foliation can have variable attitudes. Above them, the regional fabric is flat-lying to moderately dipping. It bears a generally strong stretching lineation that strikes dominantly E–W (Brun and Burg, 1982; Burg et al., 1987, 1994).

Data available to date in the area suggest that the two groups of ages observed in the metamorphic pile of the South Brittany Domain relate to two main tectonic events, as follows.

The early cooling ages observed in the upper group of units reflect early exhumation. Several lines of evidence indicate that these units emplaced by thrusting. Thus, in the Brétignolles-sur-Mer area, the porphyroids are thrust over low-grade sediments and volcanics (Ters, 1972; Iglesias and Brun, 1976; Burg, 1981; Maillet, 1984; Colchen and Poncet, 1987; Vauchez et al., 1987; Goujou, 1992) (Fig. 3a). Recently, Bosse et al. (2002) have demonstrated the occurrence of a major thrust zone within the blueschists of the Ile de Groix. At regional-scale, kinematics of these thrusting events is unclear. However, in the Brétignolles-sur-Mer area, top-to-the-West shearing is unequivocal (Brun and Burg, 1982; Vauchez et al., 1987).

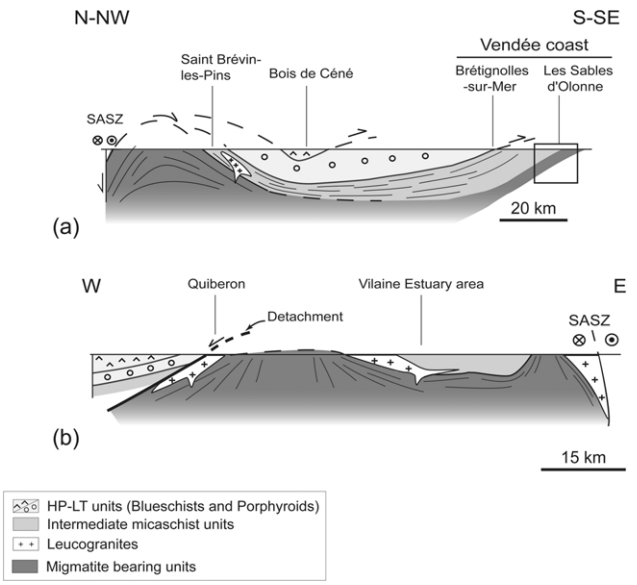

Fig. 3. Examples of cross-sections within the South Armorican Domain (locations on Fig. 2). Insert on (a) corresponds to the studied area (Fig. 4). (a) Modified after Burg (1981); (b) modified after Gapais et al. (1993).

In the Golfe du Morbihan area, it has been shown that the Quiberon leucogranite emplaced during shearing along a major normal fault zone (Gapais et al., 1993) (Fig. 3b). Gapais et al. (1993) further interpreted this as accounting for the rapid cooling of the footwall migmatites (Golfe du Morbihan) and the preservation of the Ile de Groix blueschists in the hanging wall. From structural relationships and available geochronological data, these authors concluded that there was a major extensional event during Upper-Carboniferous times. Similar relationships between upper units, synkinematic granites, and underlying high-grade units are observed in other areas of South Brittany (Vilaine Estuary and St Brévin-les-Pins areas; Fig. 3a) (Gapais et al., 1993).

3. The Sables d'Olonne area

3.1. Lithologies and metamorphism

Most sections that can be made in South Brittany across migmatite cores and overlying units show important extensional shear zones (Fig. 3b). In contrast, the coastal section of the Sables d'Olonne area shows a complete metamorphic sequence, from a migmatitic core to the South to low-grade metasediments to the North (Figs. 3a and 4) (Ters, 1972; Brillanceau, 1978; Goujou, 1992). To the North, in the Brétignolles-sur-Mer area (Fig. 3a), the top of the pile is of rather low metamorphic grade (lack of metamorphic muscovite; Goujou, 1992).

In the Sables d'Olonne area, the lithological and

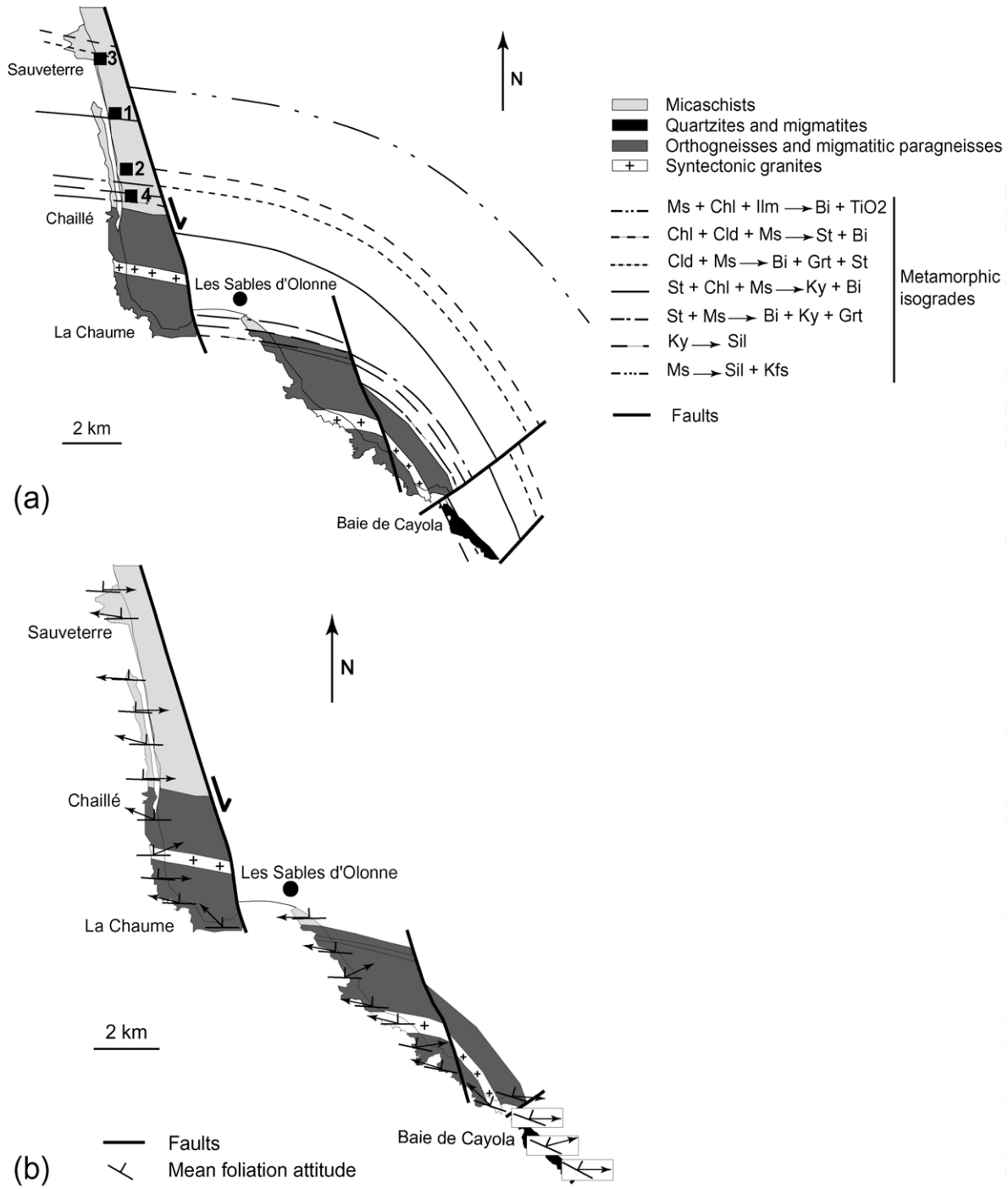

Fig. 4. (a) Geology and metamorphism of the Sables d'Olonne area (modified after Iglesias and Brun (1976) and Goujou (1992)); 1, 2, 3, and 4 are locations of P–T estimates discussed in the text. Bi, biotite; Chl, chlorite; Cld, chloritoid; Grt, garnet; ilm, illmenite; Ky, kyanite; Ms, muscovite; St, staurolite; Sil, sillimanite; Kfs, K feldspar. (b) Foliations and stretching lineations in the coastal area. Both metamorphic isograde and foliations underline the general geometry of a dome cored by migmatites.

metamorphic patterns define a dome cored by high-grade rocks, including migmatites (Fig. 4) (Goujou, 1992). The dome is locally affected by late dextral strike-slip faults that offset the metamorphic isograde (Fig. 4a).

We have focussed our study on the metamorphic part of the dome, below the biotite isograde (Fig. 4a). From top to bottom, main lithological units are as follows (Ters and Chantraine, 1980):

- Metasediments, mainly metapelites, showing a downward increase in metamorphic grade up to partial melting to the South (Fig. 4a).

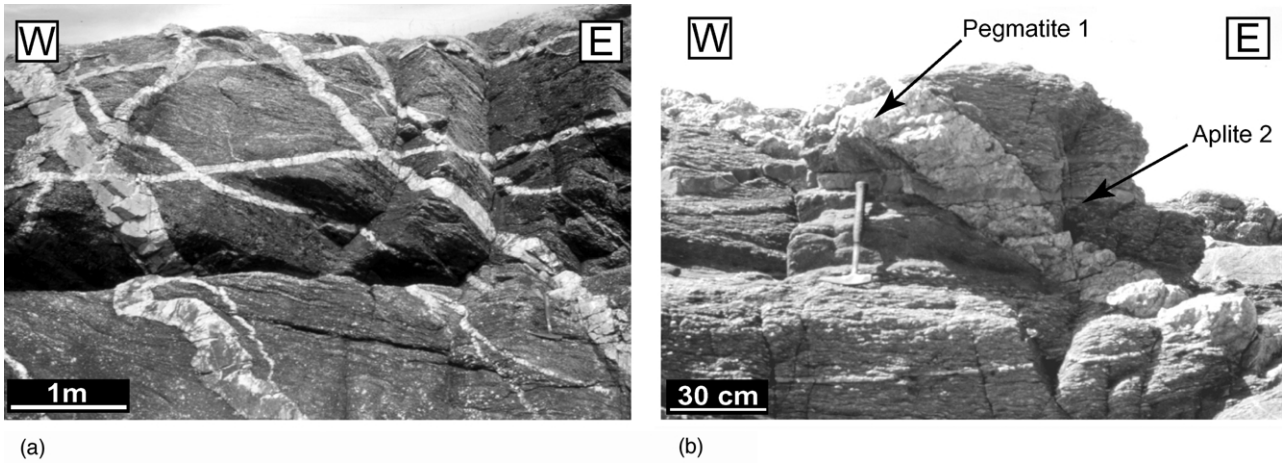

Fig. 5. General aspects of the dyke array in the Sables d'Olonne area, with numerous intrusions (a) and successive intrusions of various compositions (b).

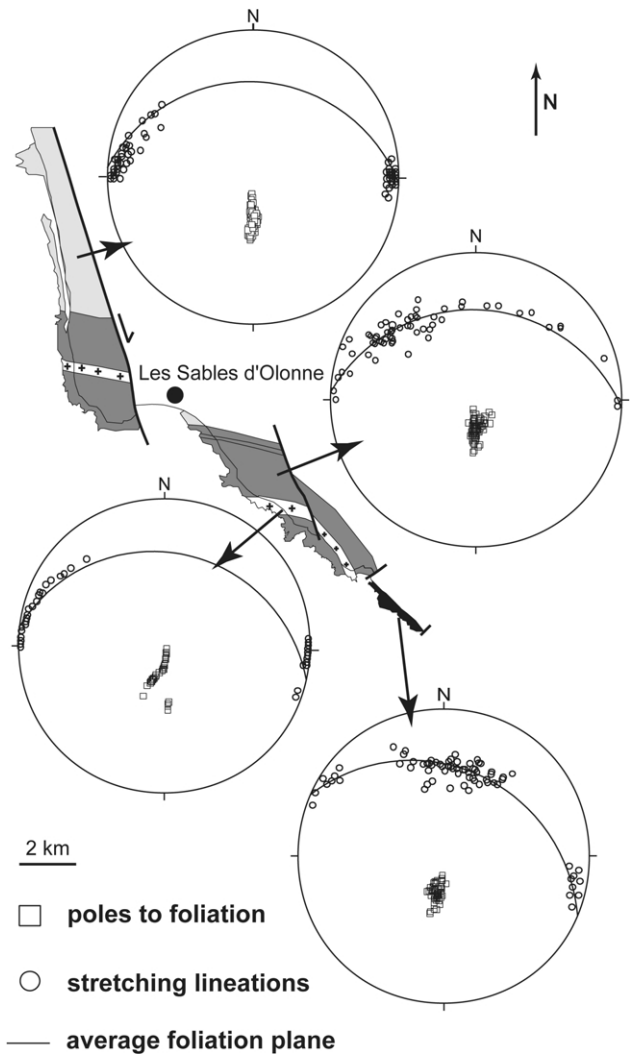

Fig. 6. Attitude of foliations and stretching lineations in the Sables d'Olonne area (equal area projections, lower hemisphere). At regional-scale, the dominant stretching lineation is E–W to WNW–ESE. Remnants of early NS-striking lineations occur at the bottom of the pile, within orthogneiss-rich and quartzite-rich units.

- Quartz-rich metasediments (including quartzites), concentrated in the migmatitic base of the metasedimentary pile (Iglesias and Brun, 1976; Cannat and Bouchez, 1986).
- Orthogneisses, mainly augengneiss with centimetre-scale phenocrysts, and migmatitic paragneisses. The transition zone between the orthogneisses and the overlying metasediments is marked by imbrications of the two lithologies.

Sheet-like intrusions of granitic material occur within the orthogneisses (Fig. 4) (Iglesias and Brun, 1976; Goujou, 1992), and a huge dyke swarm is observed within both the orthogneiss and the lower part of the metasedimentary pile (Fig. 5a). Dykes are mainly granites, pegmatites, aplopegmatites, and less commonly aplites, with clear evidence of successive injection events (Fig. 5).

3.2. Fabrics

Rocks show a metamorphic foliation whose overall attitude is consistent with the dome-shaped structure, E–W-striking and N-dipping in the northern part of the area, and WNW–ESE-striking and NE-dipping in the eastern part (Fig. 4b) (Goujou, 1992). According to Goujou (1992) and Colchen and Rolin (2001), this fabric tends to decrease in intensity toward the North, from strong and penetrative in the lower part of the pile, to more poorly developed above the biotite isograde.

The foliation bears an E–W to WNW–ESE striking stretching lineation (Iglesias and Brun, 1976) (Fig. 6). The lineation is underlined by the preferred orientation of metamorphic minerals (Goujou, 1992), and by feldspar phenocrysts and quartz ribbons in the orthogneisses. Associated shear criteria, in particular centimetre- to metre-scale shear bands that pervasively affect most rocks of the area, indicate dominant top-to-the-West motions (Brun and Burg, 1982; Goujou, 1992) (Fig. 7). Top-to-the-West shearing is also recorded by quartz fabrics (Cannat and Bouchez, 1986).

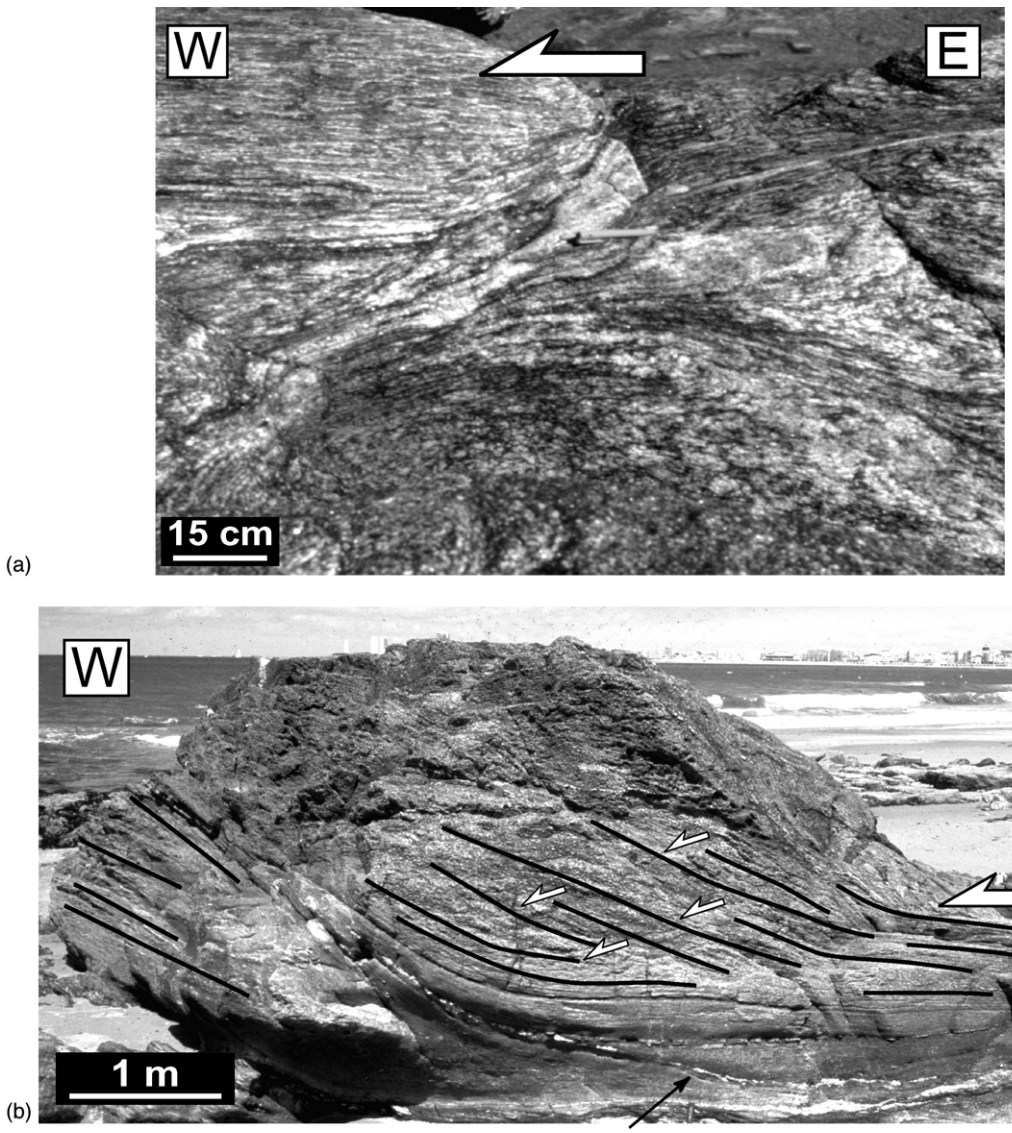

Fig. 7. Examples of top-to-the-West shear bands. (a) Metre-scale extensional shear band within orthogneisses. (b) Top-to-the-West outcrop-scale mylonitic shear zone below a lens of orthogneiss that probably suffered back rotation during shearing. Black lines underline the sigmoidal trace of the foliation. Small white arrows point out decimetre-scale shear bands. The fine black arrow points toward a quartz vein cutting across the mylonitic fabric and affected by substantial boudinage.

A N–S stretching lineation is locally observed at the base of the pile (Fig. 6). Associated shear criteria indicate top-to-the-South motions (Cannat and Bouchez, 1986). Several studies have shown that this lineation, of unknown age, is reworked by the E–W stretching (Iglesias and Brun, 1976; Brun and Burg, 1982; Cannat and Bouchez, 1986; Geoffroy, 1988, 1993). In fact, N–S lineations are best preserved within water-poor unmolten rocks of the migmatitic core, in particular within orthogneisses and quartzites (Fig. 6). Within pelitic migmatites at the bottom of the pile, stretching lineations are absent or poorly expressed. Granitic intrusions and dykes that cut-across the regional fabric are only affected by the E–W stretching (Cannat and Bouchez, 1986; Geoffroy, 1993).

4. Dyke array

4.1. Relationships between dyking and regional deformation

Field relationships show that dyke intrusions occurred during E–W stretching. Dykes cut across the foliation and show variable amounts of strain (Figs. 5, 8 and 9), consistent with successive emplacement during progressive deformation. Some dykes are free of internal fabrics, but most show a foliation consistent with that of country-rocks (Fig. 5b). Furthermore, many dykes show alignments of constitutive minerals that indicate E–W stretching (Fig. 8). In addition, dykes are commonly folded, with axial planes consistent with the regional foliation (Fig. 9a).

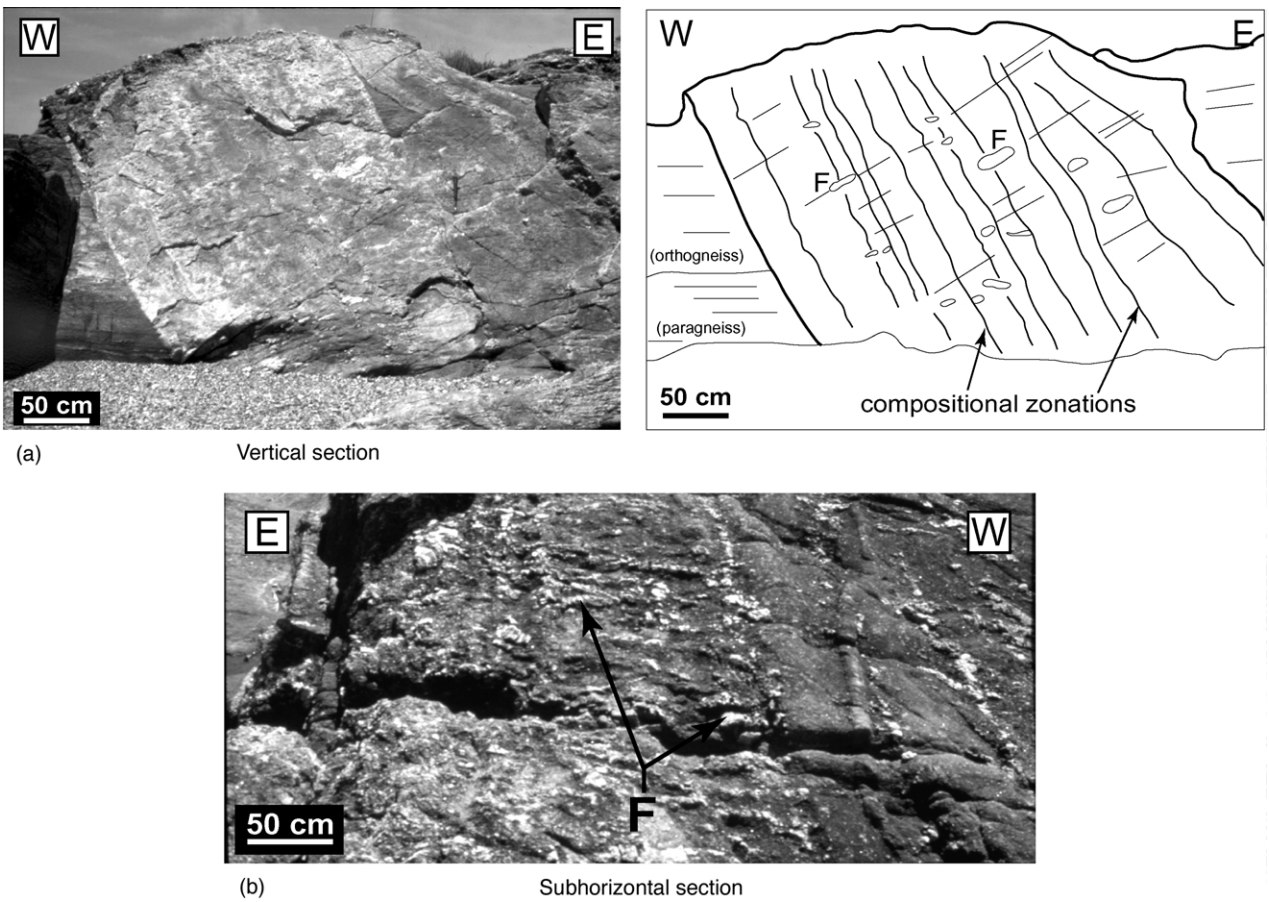

Fig. 8. Example of late dyke within orthogneissic and paragneissic country-rocks. (a) View perpendicular to foliation and parallel to stretching lineation; compositional zoning occurs parallel to dyke walls; preferred orientations of feldspar aggregates (F) underline the foliation. (b) Same dyke viewed at low angle to the foliation; feldspar-rich aggregates (F) underline the E–W stretching lineation. The overall pattern shows that the dyke emplaced by successive pulses during bulk E–W regional stretching.

Field evidence shows that dykes emplaced during dominant top-to-the-West shearing. Thus, asymmetric boudinage of stretched dykes at low angle to the regional foliation is common (Fig. 9b). In addition, folds that affect dykes are asymmetric. Their short limbs are in general West-dipping and strongly shortened, whereas their long limbs are stretched and sheared along the E–W direction (Fig. 9a). This geometry is compatible with top-to-the-West shearing. Outcrop-scale shear bands (Figs. 7 and 9b), as well as local evidence for shear localisation along reoriented dyke segments (Fig. 9a), outline the occurrence of shear strain gradients.

4.2. Geometry of the dyke array

The orientation of dykes has been measured throughout the area. Particular attention has been given to the attitude of shortened and stretched dykes (Fig. 10). Dykes or dyke segments for which the finite strain state could not be clearly assessed have not been considered in the analysis.

The strike of shortened dykes, most being folded, varies around a N–S direction (0°N ± 40°). Their dip varies strongly between 30 and 90° (Fig. 10). Poles to this set of dykes are scattered around the principal stretch direction (λ_1) defined by the regional lineation (Fig. 10). This pattern emphasizes that dyke intrusions contribute to the E–W stretching. Furthermore, the overall attitude of shortened dykes in areas where N–S lineations are well preserved also indicates E–W stretching (compare Figs. 6 and 10), which confirms that dyke intrusions post-date the N–S stretching event (Cannat and Bouchez, 1986).

Stretched dykes are generally affected by boudinage (Fig. 9b). Their strike varies around the E–W direction (90°N ± 25°) (Fig. 10). They are all gently dipping toward the North, between 10 and 40°. Their mean attitude is close to that of the regional foliation, with poles concentrated around the principal shortening direction (λ_3) (compare Figs. 6 and 10).

4.3. Dyke evolution with increasing strain

Weakly deformed dykes can show variable orientations (Fig. 5a). However, field data show that weakly deformed dykes and shortened ones are preferentially steeply dipping,

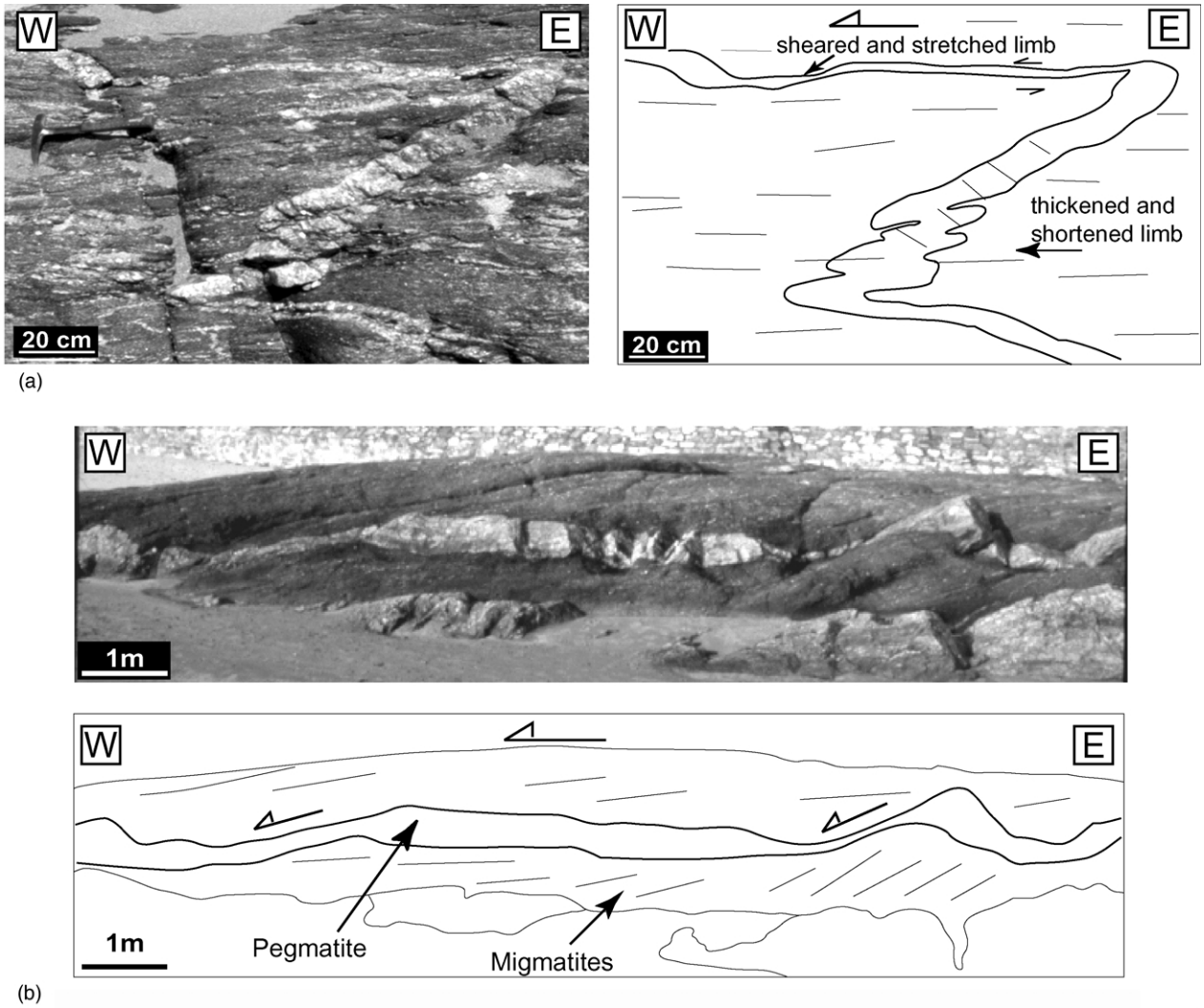

Fig. 9. Photographs illustrating syn-dyking kinematics (views at high angle to foliation and small angle to stretching lineation). (a) Example of folded granitic dyke, with shortened short limb, and stretched and sheared long limb; the overall geometry is consistent with top-to-the-West shearing. (b) Asymmetric pinch-and-swell of a granitic dyke within migmatites; the dyke cuts across the country-rock foliation, and the asymmetric boudins indicate top-to-the-West shearing.

with preferred orientations around the N–S direction (Figs. 8 and 10). Furthermore, some of these dykes show internal fabrics and compositional zoning that are consistent with progressive dyke growth during E–W stretching (Fig. 8). These features suggest that the most frequent primary dyke orientation should have been steeply-dipping and sub-meridian, which is actually consistent with E–W principal stretching. On the other hand, dykes or dyke segments that are strongly stretched lie at low angle to the regional foliation (Figs. 9 and 10), and thus appear strongly reoriented (Fig. 9a). On this basis, we have attempted to examine the possible evolution of dyke orientation with increasing strain.

To do this, we first examined relationships between the dip and strike of individual dykes. Several typical features appear on a plot of the plunge of dyke poles versus the direction of dyke poles (Fig. 11). To construct this plot, individual data are expressed within a referential frame with λ_3 vertical and λ_1 horizontal and E–W. The plot underlines that preferred orientations of folded and stretched dykes are clearly different (Fig. 11). The plot further shows that poles to stretched dykes have rather variable directions and strong plunges. In contrast, poles to shortened dykes have variable moderate plunges and show preferred directions around λ_1. The attitude of shortened or stretched segments of seven individual dykes is shown on Fig. 11 (an example of such a dyke is shown on Fig. 9a). The attitude of these segments shows a divergence in direction with respect to λ_1 when changing from shortening field to stretching field (Fig. 11). Along individual dykes, the change from shortened segments to stretched segments is very sharp (Fig. 9a). This results in a lack of poles with plunges between about 50 and 75°, irrespective of the direction (Fig. 11).

4.4. Comparison with theoretical models

In order to further examine the significance of the dyke

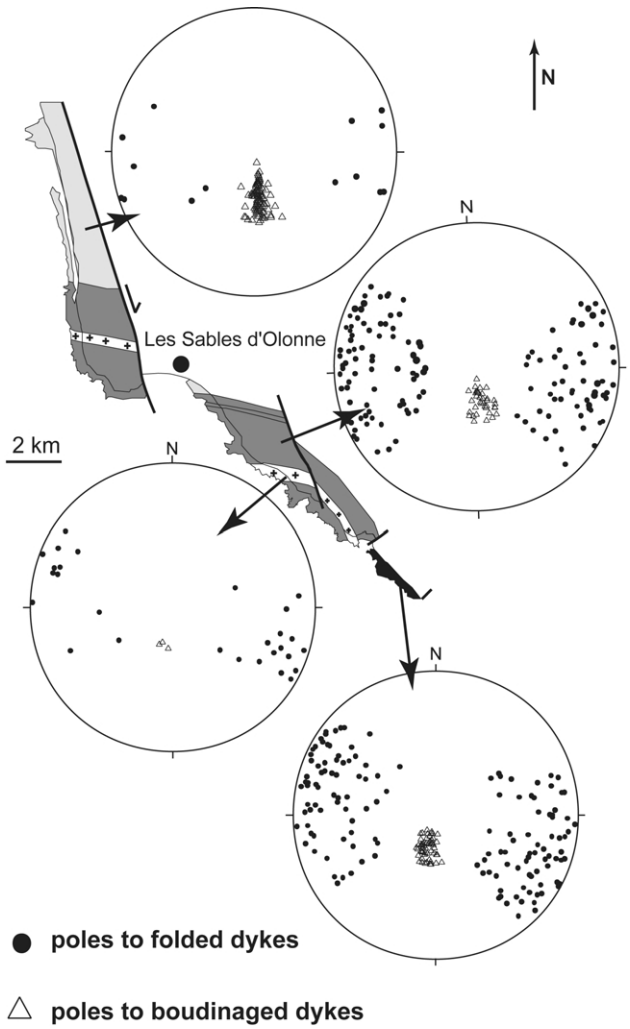

Fig. 10. General pattern of folded and stretched dykes in the Sables d'Olonne Area (equal area projections, lower hemisphere). See text for further comments.

pattern in terms of finite strain and strain regime, we have computed theoretical patterns of reoriented passive planes for different types of strain and strain history (Fig. 12).

For an easy comparison between theoretical models and field data, we used the same referential frame. For coaxial strains, models are computed with respect to a horizontal and E–W principal stretch, and a horizontal and N–S intermediate axis. For simple shear, the reference frame chosen is a horizontal shear plane and an E–W striking direction, with top-to-the-West motion. Principal strains have not been chosen as the reference frame for simple shear because no differences in patterns of passive markers between coaxial and non-coaxial histories can be imaged within such a frame. At regional scale, the overall envelope of the foliation is sub-horizontal, and foliation attitudes in the study area appear controlled by the local dome structure rather than by regional effects (Goujou, 1992) (Fig. 4). Because the dome-shaped geometry affects the isograde and the latest ductile fabric, it must be a late structure. This is why we chose to present theoretical results with respect to a horizontal frame.

For coaxial strain, equations relating the final attitude to the initial attitude of a passive plane are as follows (Ramsay, 1967, pp. 130–131, Fig. 4-5):

$$\tan\Theta'_1 = \tan\Theta_1(\lambda_3/\lambda_1)$$

$$\tan\Theta'_2 = \tan\Theta_2(\lambda_2/\lambda_1)$$

$$\tan\Theta'_3 = \tan\Theta_3(\lambda_3/\lambda_2)$$

where λ_1, λ_2, λ_3 are the principal strains, and Θ_1, Θ_2, Θ_3 and Θ'_1, Θ'_2, Θ'_3 are the initial and final angles between each principal axis and the intersection of the considered plane within the $\lambda_1\lambda_3$, $\lambda_1\lambda_2$ and $\lambda_2\lambda_3$ planes, respectively.

For simple shear, because the shear plane chosen is horizontal, the strike of rotating planes remains constant. To calculate the change in dip of planes, we have used the

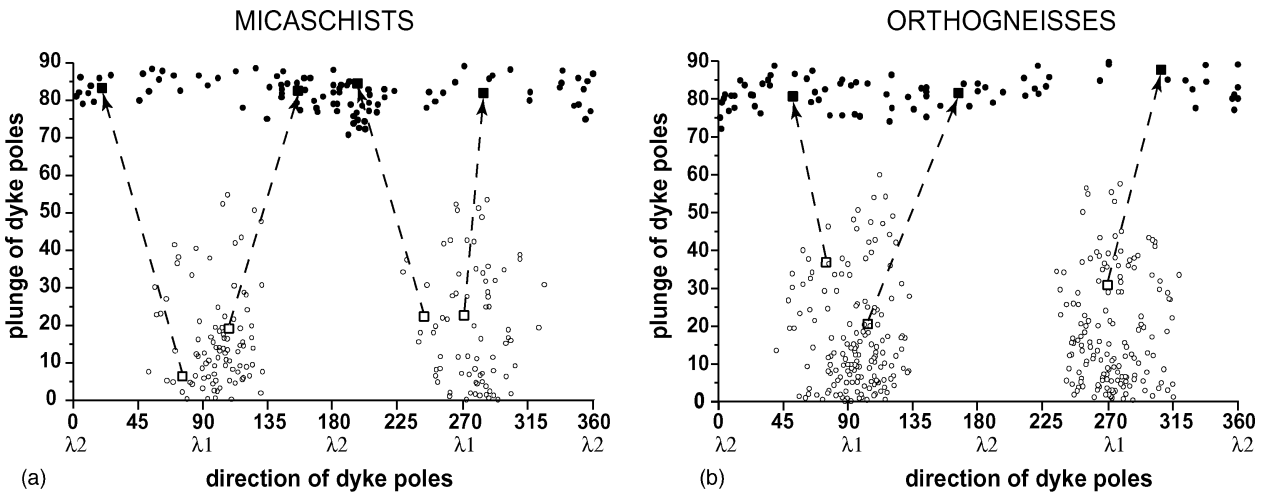

Fig. 11. Plots of plunge of dyke poles versus direction of dyke poles within micaschists (a) and orthogneisses (b); open circles are shortened dykes; black circles are stretched dykes. Changes in attitudes of dyke segments for seven individual dykes, from shortened parts (open squares) to stretched parts (black squares), sketched by arrows (precise paths are unknown). See text for further comments.

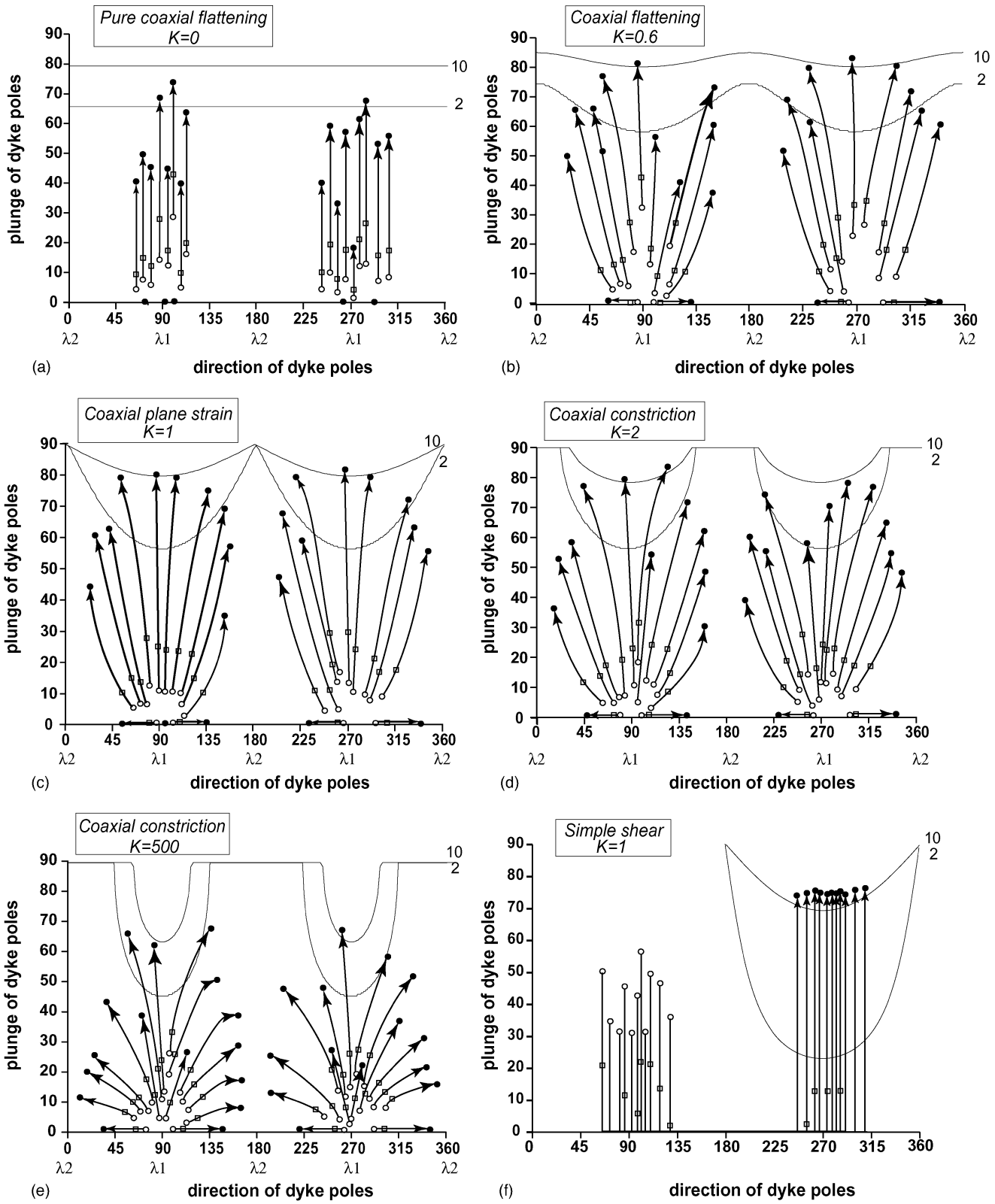

Fig. 12. Plots of plunge versus direction of poles to passive planes rotating during various deformation histories. Open and black circles are initial and final orientations ($r = 10$), respectively. Open squares are intermediate stage ($r = 2$). Boundaries between finite stretching and shortening fields are shown for $r = 2$ and $r = 10$. See text for further comments.

reorientation of the line defined by the intersection between the plane to be rotated and the plane of shear (i.e. the plane perpendicular to the shear plane and parallel to the shear direction). The rotation of such a line as a function of the shear strain γ is given by $\cot\alpha' = \cot\alpha + \gamma$ (Ramsay, 1967, p. 88, Fig. 3-23), where α' and α are the final and initial angles, respectively. After rotation, the new attitude of the pole to the considered plane is calculated using the new orientation of the intersection line and the constant strike of the plane.

For coaxial situations, we considered a set of dykes with initial orientations scattered at high angle to the principal stretch. For simple shear, the initial preferred orientation is around the perpendicular to the chosen infinitesimal stretch direction, N–S-striking and at 45° to the horizontal shear plane. For each example, the computing was run up to a strain intensity $r = 10$ ($r = \lambda_1/\lambda_2 + \lambda_2/\lambda_3 - 1$; Watterson, 1968). For simple shear, this corresponds to a shear strain γ of about 5.5.

Pure coaxial flattening ($K = 0$, with $K = (\lambda_1/\lambda_2 - 1)/(\lambda_2/\lambda_3 - 1)$; Flinn, 1962) imposes that the direction of poles remains constant with increasing strains (Fig. 12a).

For strain ellipsoids with shapes around plane strain, the path of poles have divergent shapes with increasing strain. Poles initially close to λ_1 move toward the $\lambda_2\lambda_3$ plane, and their plunge increases strongly (Fig. 12b–d).

For strongly constrictive coaxial strains, divergent paths are also observed, but the change in the plunge of poles is much less pronounced than for the other types of strain ellipsoids (Fig. 12e).

For comparison, Fig. 12f illustrates a simple shear applied to a set of planes initially concentrated at 45° to the shear plane. The plot underlines that all planes converge rapidly toward the bulk shear plane. Because of the choice of a horizontal shear plane, their direction remains constant. As the simple shear model imposes a westward-directed shear, all poles to planes reach directions exceeding 180°N (i.e. all planes dip eastward) after a moderate amount of shear. Among the different examples tested, the only deformation history for which planes are all rapidly reoriented within the stretching field of the strain ellipsoid is simple shear (Fig. 12).

From the comparison between field data (Fig. 11) and theoretical models (Fig. 12), we make the following inferences:

- The observed dyke pattern cannot result from simple shear alone.
- Strongly constrictive or flattening coaxial strains do not account for the observed dyke pattern.
- The combined increase in plunge and direction divergence with increasing strain is best explained by coaxial strains involving moderate stretching or shortening along the intermediate principal strain axis (strain ellipsoids around plane strain).
- The strong reorientation of all stretched dykes (Fig. 11) is best explained by a substantial component of simple shearing.

5. Discussion

5.1. Shape of the finite strain ellipsoid

Models of reorientation of passive planes do not allow us to estimate the precise shape of the finite strain ellipsoid, between either moderately flattened or moderately constricted (compare Figs. 11 and 12b–d). However, dyke patterns with poles to stretched dykes concentrated along λ_3 are expected in the flattening field (see Ramsay, 1967, pp. 154–156; Talbot, 1970, Figs. 3 and 4). Flattening strain is actually supported by microstructural observations. In particular, Iglesias and Brun (1976) have described shadow zones around synkinematic biotite porphyroblasts, with crystallizations along the λ_2 axis. We could not go further in the analysis of the dyke pattern in terms of type of strain ellipsoid. Indeed, the systematic lack of data between zones of stretched and shortened dykes (Fig. 10) does not allow the precise location of the surface of no finite longitudinal strain. Therefore, the estimate of the 'minimum strain ellipsoid' using dykes (Talbot, 1970) cannot be applied here.

5.2. Progressive deformation of dykes

The analysis above shows that the dyke pattern can be explained by a deformation combining top-to-the-West shearing and coaxial shortening, and affecting dykes most probably injected along steeply-dipping and sub-meridian directions. Furthermore, field evidence shows that injections occurred at various stages during the deformation history. These features imply a substantial component of coaxial strain. Indeed, they reflect different intrusion stages at high angle to the finite principal stretch direction, which is not compatible with simple shear only. Consistently, directions of poles to dykes reoriented toward the foliation are strongly scattered, between 0°N and 360°N (Fig. 11). This is expected for coaxial strains (Fig. 12b–d) where planes can rotate westward or eastward according to their initial attitude. For a top-to-the-West simple shear, most, or even all, directions of poles to reoriented dykes should exceed 180°N (Fig. 12f).

In our analysis, we have compared dykes with passive markers rotating during progressive deformation. This is, of course, a strong simplification of what occurs in natural situations. Indeed, viscosity contrasts exist between dykes and country-rocks. During injection and onset of cooling, a strong negative viscosity contrast exists between molten dyke and country-rocks; whereas once solid-state is reached, one expects a positive viscosity contrast between dykes and country-rocks because of differences in

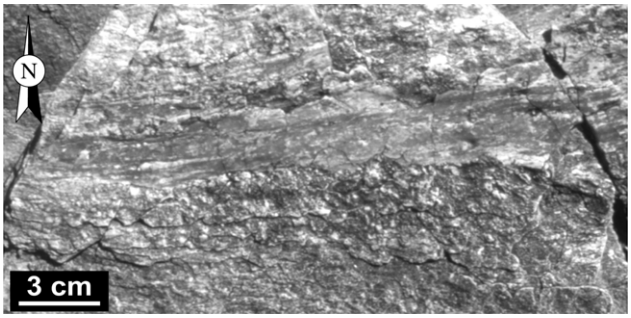

Fig. 13. Photograph of a dyke strongly mylonitised and at low angle to the regional foliation (map-view parallel to the foliation). Quartz–feldspar ribbons underline the E–W stretching lineation.

composition (especially mica content; see Bos et al., 2000) and grain size (especially for pegmatites).

Field evidence indicates that viscosity contrasts between dykes and country-rocks remained generally moderate during ductile deformation of the dykes. Thus, some dykes at high angle to the foliation are thickened but not folded, which indicates a negligible viscosity contrast. Others show cleavage refractions, indicating positive viscosity contrasts. However, most stretched dykes are affected by pinch-and-swell rather than by boudinage (Fig. 9b), which shows that positive viscosity contrasts remained moderate. Cuspate folds are never seen, suggesting that rapid cooling of the dykes limited the existence of strong negative viscosity contrasts.

A peculiar feature of the dyke pattern is the sharp transition between shortened and stretched dyke segments (Figs. 9a and 11). This could be in part due to the simple shear component that induced rapid dyke rotations. However, many dyke segments at low angle to the foliation show evidence of localised parallel shearing (Fig. 9a). Such dyke segments can be strongly mylonitised as a result of localised shearing (Fig. 13). From this, we infer that there should be some critical degree of dyke reorientation above which dykes can act as active shear surfaces, provided the viscosity contrast with country-rocks remains sufficiently low. Theoretical studies and analogue models have shown that efficient shear zones or faults tend to track orientations along which a minimum stretch and a maximum amount of shear strain are accumulated (Gapais et al., 1987, 1991). Thus, with respect to the bulk strain ellipsoid, such zones tend to show preferred orientations between directions of no finite extension and directions of maximum amount of shear. Simple shear sand-box experiments on brittle faulting have shown that faults initially created at 15° to the principal compressive stress (Mohr–Coulomb criterion) became reoriented toward directions of maximum shear and minimum stretch for rather small amounts of shear strain (γ around 0.5) (Gapais et al., 1991). A similar behaviour could account for the lack of dykes showing intermediate dips (Fig. 11). The simple shear component of the deformation, acting on non-passive dykes, would thus be the main reason why strain analysis using the minimum strain ellipsoid method (Talbot, 1970) could not be applied here.

5.3. Estimates of amounts of vertical thinning

The occurrence of a substantial component of coaxial strain associated with the development of a flat-lying to moderately dipping foliation implies sub-vertical shortening, and therefore crustal thinning.

An estimate of the maximum coaxial shortening recorded by the dyke array can be made using mean initial and final attitudes of reoriented dykes. Models for passive planes indicate that strain intensities r of at least 10 are required to rotate dykes within the stretch field of the strain ellipsoid (Fig. 12). The corresponding amount of shortening is around 80% (λ_3 around 0.20). However, an r value around 10 is probably a maximum one because (1) there is evidence for non-passive behaviour of dykes, (2) there is a simple shear component, and (3) fold geometries with strongly sheared long limbs reflect heterogeneous strain.

Goujou (1992) has argued that the Barrovian metamorphism was the consequence of crustal thickening. On the other hand, metamorphic minerals are associated with the development of the regional foliation (Goujou, 1992), and our analysis of late dykes shows that this fabric reflects extensional deformation. This apparent contradiction suggests that the initial Barrovian metamorphic gradient has been modified during extension. Consistently, metamorphic minerals such as biotite porphyroblasts commonly show internal deformations and are wrapped by the dominant foliation, indicating growth during early deformation stages (Iglesias and Brun, 1976, Fig. 2). The present-day metamorphic gradient should thus provide an estimate of the amount of syn-extension shortening. Four particular locations of PT estimates are shown on Fig. 4a. At location 1, Goujou (1992) has estimated temperatures between 575 and 585 °C, assuming that associated pressures were comprised between 350 and 600 MPa. At location 2, Goujou (1992) calculated equilibrium PT conditions of 700 ± 30 °C and 770 ± 100 MPa, using the assemblage Bi + St + Ky + Grt_{FeMn}. Locations 3 and 4 correspond to the Grt + (Cld + Ms → Bi + Grt + St) and the Sil + (Ky → Sil) isograds, respectively. Reasonable PT conditions at these locations are around 450 ± 50 °C for 400 ± 100 MPa and 600 ± 50 °C for 800 ± 100 MPa, respectively (see Bucher and Frey, 1994).

No evidence for important normal faults that could have reduced the thickness of the metamorphic pile is observed along the studied section. Therefore, using the average attitude of the foliation, and assuming that isograds are parallel to the foliation and that peaks in pressure are synchronous at different locations, one can estimate a maximum amount of bulk shortening. For a mean foliation dip of 30°, locations 1 and 2 yield around 90% shortening. The other pair of localities yields about 75% shortening.

The lowest amount of shortening, of the order of 75%,

can be compared with temperature estimated at the four localities in order to estimate a possible pre-extension thermal gradient. For localities 1 and 2 (1 km apart, for a mean foliation dip of 30°) and 3 and 4 (1.9 km apart), estimated thermal gradients are of the order of 30° km^{-1} and 20° km^{-1}, respectively. These values appear somewhat lower than those classically invoked for a Barrovian gradient (generally given around 30–35° km). This confirms that the range of shortening estimates is probably a maximum.

5.4. Extension mechanism

The occurrence of sub-vertical shortening throughout the metamorphic pile of the Sables d'Olonne area attests to crustal thinning. This deformation, which is of Upper Carboniferous age (Colchen and Poncet, 1987; Goujou, 1992; Colchen and Rolin, 2001), was previously interpreted as related to nappe emplacement during compressive tectonics. However, extension has also been invoked (Gapais et al., 1993; Burg et al., 1994; Colchen and Rolin, 2001). Our study and its comparison with other areas of South Brittany (Gapais et al., 1993) (Fig. 3) demonstrate that the observed deformation results from extensional tectonics.

According to the estimates of maximum shortening, the pre-extension pile between the biotite and the sillimanite isograds was of the order of 10 km thick. Moving upward in the metamorphic pile, the amount of strain associated with late ductile deformations decreases (Goujou, 1992; Colchen and Rolin, 2001). We interpret this as a downward increase of extensional strains associated with increasing thermal conditions. Consistently, in the Brétignolles-sur-Mer area, the low-grade upper-crustal metasediments that constitute the top of the pile do not show clear evidence of important extensional structures (Colchen and Poncet, 1987; Goujou, 1992; Colchen and Rolin, 2001). In fact, most structures in this area can be attributed to the thrusting of the overlying Vendée Porphyroids (Iglesias and Brun, 1976; Brun and Burg, 1982; Goujou, 1992). This tectonic event occurred during the Lower Carboniferous (Le Hébel, 2002), and thus pre-dates extension. From these, we infer that the syn-extension brittle–ductile transition was located somewhere around the Brétignolles-sur-Mer area. The southward increase in strain from Brétignolles-sur-Mer to the Sables d'Olonne suggests that extension has been accommodated by bulk heterogeneous shearing and thinning of the weak metamorphic pile (Fig. 14).

Several domes similar to the Sables d'Olonne dome occur in Vendée (Goujou, 1992). Around the dome of La Roche-sur-Yon (Fig. 2), apparent thermal gradients of up to 70–80° km^{-1} are observed (Goujou, 1992), and we interpret this as due to crustal thinning above an extensional dome. Migmatite domes of Vendée show several particular features compared with other extensional uplifts of migmatites observed in South Brittany.

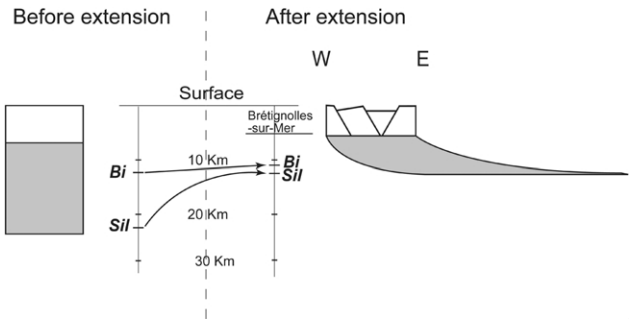

Fig. 14. Cartoon illustrating the overall change in shape of the metamorphic pile of the Sables d'Olonne area by combination of heterogeneous vertical shortening and horizontal simple shear during Upper Carboniferous extension. See text for further comments.

For example, in the Quiberon area, most of the extension appears accommodated by a normal shear zone (Fig. 3b) that cuts across the micaschists (Gapais et al., 1993). Consistently, the thickness of the micaschist pile above the migmatites is much reduced compared with that of the Sables d'Olonne area, and migmatites are uplifted close to the porphyroids, i.e. close to the brittle–ductile transition. In the footwall of the Quiberon shear zone, migmatites are marked by steeply-dipping, N–S-striking foliations (Audren, 1987). In contrast, foliations observed within the Vendée migmatites are flat-lying, parallel to those observed in the overlying micaschists. Thus, the Quiberon area has an overall core-complex geometry, the steep attitude of foliations within migmatites being possibly due to some roll-under effect (Brun and Van Den Driessche, 1994); whereas the Sables d'Olonne area looks like a deformation zone where pervasive crustal thinning accommodates most of the extension. However, the occurrence of local décollements associated with flat-and-ramp structures cannot be ruled out. This is indeed suggested by outcrop-scale evidence of shear localisation (Figs. 7, 9b and 13).

Analogue models suggest that the formation of a detachment and associated core-complex requires rather local weak heterogeneities within the ductile thickened crust (e.g. a highly molten zone) (Brun et al., 1994). Without such heterogeneity, distributed thinning is observed in experiments (Brun et al., 1994). The extension pattern observed in the Sables d'Olonne area could thus reflect a local lack of strong and large heterogeneities of viscosities. Another hypothesis could be that the area reflects the extensional pattern that predates strain localisation along detachments. Indeed, the overall crustal cooling expected to occur during thinning could induce increasing strain localisation during progressive extension. On the other hand, according to available geochronological data (Goujou, 1992; Brown and Dallmeyer, 1996), the formation of the Quiberon detachment is coeval with the extensional pattern observed in the Sables d'Olonne. It is thus more probable that this latter area

reflects large and distributed crustal thinning occurring between core complexes.

6. Conclusions

From the above analysis, we draw the following conclusions:

1. The latest event of major ductile deformation observed in the Sables d'Olonne area is due to crustal extension. From the analogy between this area and the rest of the high-grade metamorphic Vendée, this conclusion can be extended at regional scale. This emphasizes the importance of Upper Carboniferous extension in the South Brittany Domain.
2. The extension pattern is that of pervasive crustal thinning, without evidence of important detachment zones. This could correspond to extensional patterns occurring between the core complex.
3. Crustal thinning was accommodated by combined coaxial shortening and top-to-the-West shearing.
4. The maximum amount of thinning is of the order of 80%.
5. Extension has been documented by the analysis of the pattern of a syn-kinematic dyke array. This work confirms that the analysis of such structures can be powerful to constrain finite strains and kinematics of a deformed zone.

Acknowledgements

This work is an MSc project (F.C.) developed in the course of the Armor 2 project (Géofrance 3D Program, BRGM-INSUE). The paper benefited from constructive discussions with M. Ballèvre, R. Capdevila, P. Gautier and P. Pitra. Suggestions of two anonymous reviewers helped in preparing the last version of the paper.

References

Audren, C., 1987. Evolution structurale de la Bretagne méridionale au Paléozoïque. Mémoires de la Société Géologique et Minéralogique de Bretagne 31.

Bernard-Griffiths, J., Peucat, J.J., Sheppard, S., Vidal, P., 1985. Petrogenesis of Hercynian leucogranites from South Armorican massif. Contributions of REE and isotopic (Sr, Nd, Pb, O) geochemical data to the study of source rock characteristics and ages. Earth and Planetary Science Letters 74, 235–250.

Bos, B., Peach, C.J., Spiers, C.J., 2000. Frictional-viscous flow of simulated fault gouge caused by the combined effects of phyllosilicates and pressure solution. Tectonophysics 327, 173–194.

Bosse, V., Ballèvre, M., Vidal, O., 2002. Ductile thrusting recorded by the garnet isograd from the blueschist-facies metapelites of the Ile de Groix, Armorican Massif, France. Journal of Petrology 43, 485–510.

Brillanceau, A., 1978. Guide Géologique Régional Poitou-Vendée-Charente, Masson, Paris.

Brown, M.D., Dallmeyer, R.D., 1996. Rapid Variscan exhumation and the role of magma in core complex formation: southern Brittany metamorphic belt, France. Journal of Metamorphic Geology 14, 361–379.

Brun, J.P., Burg, J.P., 1982. Combined thrusting and wrenching in the Ibero–Armorican arc: a corner effect during continental collision. Earth Planetary Science Letters 61, 319–332.

Brun, J.P., Van Den Driessche, J., 1994. Extensional gneiss domes and detachment faults systems: structure and kinematics. Bulletin de la Société Géologique de France 165 (6), 519–530.

Brun, J.P., Sokoutis, D., Van Den Driessche, J., 1994. Analogue modeling of detachment faults systems and core complexes. Geology 22, 319–322.

Bucher, K., Frey, M., 1994. Petrogenesis of Metamorphic Rocks, Springer Verlag, Berlin, Heidelberg.

Buck, W.R., 1991. Modes of continental lithospheric extension. Journal of Geophysical Research 96, 20161–20178.

Burg, J.P., 1981. Tectonique tangentielle hercynienne en Vendée littorale: signification des linéations E–W dans les porphyroïdes à foliation horizontale. Comptes Rendus de l'Académie des Sciences de Paris (série II) 293, 849–854.

Burg, J.P., Balé, P., Brun, J.P., Girardeau, J., 1987. Stretching lineations and transport direction in the Ibero–Armorican arc during the Siluro–Devonian collision. Geodinamica Acta 1, 71–87.

Burg, J.P., Van Den Driessche, J., Brun, J.P., 1994. Syn-to post thickening in the Variscan Belt of the Western Europe: modes and structural consequences. Géologie de la France 3, 33–51.

Cannat, M., Bouchez, J.L., 1986. Linéations N–S et E–W en Vendée littorale (Massif Armoricain). Episodes tangentiels successifs éo-hercyniens en France occidentale. Bulletin de la Société Géologique de France 16, 299–310.

Colchen, M., Poncet, D., 1987. Sur l'âge post-Tournaisien de la tectonique hercynienne syn-schisteuse à Brétignolles-sur-Mer-sur-Mer, Vendée littorale, Massif Armoricain. Comptes Rendus de l'Académie des Sciences de Paris (série II) 305, 1255–1258.

Colchen, M., Rolin, P., 2001. La chaîne hercynienne en Vendée. Géologie de la France 1-2, 53–85.

Coney, P.J., Harms, T.A., 1984. Cordilleran metamorphic core complexes: Cenozoic extensional relics of Mesozoic compression. Geology 12, 550–554.

Crittenden, M.D., Coney, P.J., Davis, G.H. (Eds.), 1980. Cordilleran Metamorphic Core Complexes. Geological Society of America Memoir 153.

Davis, G.H., Coney, P.J., 1979. Geological development of Cordilleran metamorphic core complexes. Geology 7, 120–124.

England, P.C., Thompson, A.B., 1984. Pressure–temperature–time paths of regional metamorphism, I. Heat transfer during the evolution of regions of thickened continental crust. Journal of Petrology 25, 894–908.

Escher, A., Watterson, J., 1974. Stretching fabrics, folds and crustal shortening. Tectonophysics 22, 223–231.

Escher, A., Escher, J.C., Watterson, J., 1975. The reorientation of the Kangâmiut Die Swarm, West Greenland. Canadian Journal of Earth Sciences 12, 158–173.

Flinn, D., 1962. On folding during three-dimensional progressive deformation. Journal of the Geological Society of London 118, 385–428.

Gapais, D., Balé, P., Choukroune, P., Cobbold, P.R., Mahjoub, Y., Marquer, D., 1987. Bulk kinematics from shear zone patterns: some field examples. Journal of Structural Geology 9, 635–646.

Gapais, D., Fiquet, G., Cobbold, P.R., 1991. Slip system domains, 3. New insights in fault kinematics from plane-strain sandbox experiments. Tectonophysics 188, 143–157.

Gapais, D., Lagarde, J.L., Le Corre, C., Audren, C., Jégouzo, P., Casas Sainz, A., Van Den Driessche, J., 1993. La zone de cisaillement de Quiberon: témoin d'extension de la chaîne varisque en Bretagne méridionale au Carbonifère. Comptes Rendus de l'Académie des Sciences de Paris (série II) 316, 1123–1129.

Geoffroy, L., 1988. Histoire de la déformation dans les métamorphites de Sauveterre. Vendée littorale. Comptes Rendus de l'Académie des Sciences de Paris (série II) 307, 277–280.

Geoffroy, L., 1993. Tectonique tardi-varisque en failles normales ductiles en Vendée Littorale. Massif Armoricain. Comptes Rendus de l'Académie des Sciences de Paris (série II) 317, 1237–1243.

Goujou, J.C., 1992. Analyse pétro-structurale dans un avant-pays métamorphique: influence du plutonisme tardi-orogénique varisque sur l'encaissant épi à mésozonal de Vendée. Document du Bureau de Recherche Géologique et Minière 216.

Iglesias, M., Brun, J.P., 1976. Signification des variations et anomalies de la déformation dans un segment de la chaîne hercynienne (les séries cristallophylliennes de la Vendée littorale, Massif Armoricain). Bulletin de la Société Géologique de France 7, 1443–1452.

Jégouzo, P., 1980. The South Armorican Shear Zone. Journal of Structural Geology 2, 39–47.

Jones, K.A., Brown, M., 1990. High-temperature "clockwise" P–T paths and melting in the development of regional migmatites: an example from Southern Brittany, France. Journal of Metamorphic Geology 14, 361–379.

Kliegfield, R., Crespi, J., 1984. Displacement and strain patterns of extensional orogens. Tectonics 3, 577–609.

Le Corre, C., Auvray, B., Ballèvre, M., Robardet, M., 1991. Le Massif armoricain. Bulletin de la Société Géologique de France 44, 31–103.

Le Hébel, F., 2002. Déformation continentale et histoire des fluides au cours d'un cycle subduction, exhumation, extension. Exemples des porphyroïdes sud-armoricains. Ph.D. thesis, Université de Rennes.

Le Hébel, F., Vidal, O., Kienast, J.R., Gapais, D., 2002. Les porphyroïdes de Bretagne méridionale: une unité de HP–BT dans la chaîne hercynienne. Comptes Rendus de Géoscience 334, 205–211.

Maillet, D., 1984. Relations des porphyroïdes et des schistes de Saint-Gilles avec les formations siluriennes de Brétignolles-sur-Mer-sur-Mer (Vendée maritime). Une tectonique tangentielle par cisaillement ductile pendant l'orogenèse acadienne. Ph.D. thesis, Université d'Aix-Marseille.

Passchier, C.W., 1990. Reconstruction of deformation and flow parameters from deformed vein sets. Tectonophysics 180, 185–199.

Ramsay, J.G., 1967. Folding and Fracturing of Rocks, McGraw-Hill, New York.

Sonder, L.J., England, P.C., Wernicke, B.P., Christiansen, R.L., 1987. A physical model for Cenozoic extension of western North America. In: Coward, R.J., Dewey, J.F., Hancock, P.L. (Eds.), Continental Extensional Tectonics. Geological Society Special Publication 28, pp. 187–201.

Talbot, C.J., 1970. The minimum strain ellipsoid using deformed quartz veins. Tectonophysics 9, 47–76.

Ters, M., 1972. Sur l'extension du paléozoïque en Vendée littorale. Stratigraphie et structure. Compte Rendu sommaire de la Société Géologique de France 3, 1146–1148.

Ters, M., Chantraine, J., 1980. Le métamorphisme éo-dévonien dans le Sud–Est du Massif Armoricain: La coupe des Sables d'Olonne (Vendée). Livret guide pour l'excursion B03 du 26ème Congrès Géologique International, France, introduction à la géologie de la France.

Triboulet, C., Audren, C., 1988. Controls of P–T–t deformation path from amphibole zonation during progressive metamorphism of basic rocks (estuary of the River Vilaine, South Brittany, France). Journal of Metamorphic Geology 6, 117–133.

Vauchez, A., Maillet, D., Sougy, J., 1987. Strain and deformation mechanisms in the Variscan nappes of Vendée South Brittany, France. Journal of Structural Geology 9, 31–40.

Watterson, J., 1968. Homogeneous deformation of the gneisses of Vesterland, South-West Greenland. Grønlands Geologiske Undersøgelse 175, 1–78.